

Chaotic Scattering and Capture of Strings by Black Hole

Andrei V. Frolov^{*†} and Arne L. Larsen^{‡§}

^{*} *Physics Department, University of Alberta
Edmonton, Alberta, Canada, T6G 2J1*

[‡] *Physics Department, University of Odense
Campusvej 55, 5230 Odense M, Denmark
(August 11, 1999)*

Abstract

We consider scattering and capture of circular cosmic strings by a Schwarzschild black hole. Although being a priori a very simple axially symmetric two-body problem, it shows all the features of chaotic scattering. In particular, it contains a fractal set of unstable periodic solutions; a so-called strange repeller. We study the different types of trajectories and obtain the fractal dimension of the basin-boundary separating the space of initial conditions according to the different asymptotic outcomes. We also consider the fractal dimension as a function of energy, and discuss the transition from order to chaos.

PACS numbers: 04.70.-s, 04.25.Dm, 05.45.Ac, 05.45.Df

Typeset using REVTeX

[†]Electronic address: andrei@phys.ualberta.ca

[§]Electronic address: all@fysik.ou.dk

Chaos in general relativity and cosmology is by now a well-established subject. Some studies, pioneered by the work of Hawking [1] and Page [2], have been concerned with the behavior of solutions to the Einstein equations themselves; the most famous example now being the mixmaster universe (see for instance [3], and references given therein). In other studies, the subject of interest has been the behavior of test-particle trajectories in black hole spacetimes (see for instance [4,5]). In the latter case, since point-particle motion is completely integrable in the generic Kerr-Newman background [6], it was necessary to consider quite complicated multi black hole spacetimes (typically of the Majumdar-Papapetrou type [7,8]) to obtain chaotic point-particle dynamics. Taking into account that these systems represent (at least) three-body problems, and comparing with Newtonian dynamics, it was certainly no surprise that chaotic dynamics appeared. (It should be mentioned, however, that in the two black hole case, chaos is really a relativistic effect [4].) The main interest in these systems therefore was also to use and further develop coordinate-invariant descriptions and measures of chaotic behavior [9,10], suitable for general relativity where space and time are not absolute.

In the present paper, we study a conceptually simpler and more symmetric system in general relativity that nevertheless, and maybe somewhat surprisingly, leads to chaotic behavior. We consider the two-body problem of a circular test-string in the background of a Schwarzschild black hole. The circular string is taken to be coaxial with the black hole and is allowed to oscillate in its plane and to propagate in the direction perpendicular to its plane, as illustrated in Fig. 1. The combined system is therefore axially symmetric.

The physical picture we have in mind is that of a cosmic string nearby an astrophysical black hole. For a GUT string with string tension of the order $G\mu \approx 10^{-6}$ [11], the test-string approximation should be valid even for a string initially up to (say) 10^4 times longer than the black hole horizon radius. Moreover, for a GUT string we can use the leading order thickness approximation, where the cosmic string is described by the Nambu-Goto action [11]

$$S = -\mu \int d\tau d\sigma \sqrt{-\det[G_{ab}]}, \quad (1)$$

where $G_{ab} = g_{\mu\nu} X_{,a}^{\mu} X_{,b}^{\nu}$ is the induced metric on the string worldsheet. In this case, the string equations of motion and constraints (in conformal gauge) take the standard form

$$\ddot{X}^{\mu} - X''^{\mu} + \Gamma_{\rho\sigma}^{\mu} (\dot{X}^{\rho} \dot{X}^{\sigma} - X'^{\rho} X'^{\sigma}) = 0, \quad (2)$$

$$g_{\mu\nu} \dot{X}^{\mu} \dot{X}^{\nu} = g_{\mu\nu} (X'^{\mu} X'^{\nu} + X'^{\mu} X'^{\nu}) = 0, \quad (3)$$

where dot $\dot{}$ and prime \prime denote derivatives with respect to string worldsheet coordinates τ and σ . Using Schwarzschild coordinates for the background metric

$$ds^2 = -\left(1 - \frac{2M}{r}\right) dt^2 + \left(1 - \frac{2M}{r}\right)^{-1} dr^2 + r^2 d\Omega^2, \quad (4)$$

and parameterizing the circular string by ansatz

$$t = t(\tau), \quad r = r(\tau), \quad \theta = \theta(\tau), \quad \phi = \sigma, \quad (5)$$

one finds that the string equations of motion (2) and constraints (3) lead to the following system of ordinary differential equations

$$\dot{t} = E \left(1 - \frac{2M}{r}\right)^{-1}, \quad (6)$$

$$\ddot{r} = (r - 3M)\dot{\theta}^2 - (r - M)\sin^2 \theta, \quad (7)$$

$$\ddot{\theta} = -\frac{2}{r}\dot{r}\dot{\theta} - \sin \theta \cos \theta, \quad (8)$$

supplemented by the constraint

$$\dot{r}^2 + (r^2 - 2Mr)(\dot{\theta}^2 + \sin^2 \theta) = E^2. \quad (9)$$

The integration constant E , appearing here, will play the role of external control parameter (“order parameter”) for the system. It is equal to the total conserved energy of the string divided by $2\pi\mu$. In the absence of first integrals other than (9), we are thus dealing with a three-dimensional phase space. Notice also that the worldsheet time τ is not equal to the proper time. The worldsheet time τ is however finite for a string falling into the black hole.

Eqs. (6–9) are equivalent to the following Hamiltonian system

$$H = \frac{1}{2} \left(1 - \frac{2M}{r}\right) P_r^2 + \frac{1}{2r^2} P_\theta^2 - \frac{E^2}{2} \left(1 - \frac{2M}{r}\right)^{-1} + \frac{1}{2} r^2 \sin^2 \theta, \quad (10)$$

with the constraint $H = 0$. This is very similar to the Hamiltonian describing zero angular momentum photons in the Schwarzschild background [12], except for the last term in the potential which is due to the string tension. This is precisely the term that leads to non-integrability and, as we shall see, chaos.

The Hamiltonian system (10) has been previously considered and solved in the equatorial plane ($\theta = \pi/2$) [13], and some trajectories in the general case were computed numerically in [14]. In this paper, we make a more complete analysis of the dynamics associated with the Hamiltonian (10). In particular, we shall demonstrate the presence of chaos in this simple system.

Due to the non-integrable nature of the dynamical system (6–9), the analysis of the string evolution was done numerically. The string trajectories for various initial conditions were obtained by integrating Eqs. (7) and (8) using the fifth order embedded Runge-Kutta method with adaptive step size control [15]. The constraint (9) was used to independently check for numerical precision.

It is easy to see that there are three possible asymptotic outcomes of the string dynamics. The string can either fly by the black hole and escape to $(r, \theta) = (\infty, \pi)$, or the string can backscatter and escape to $(r, \theta) = (\infty, 0)$, or the string can be captured by the black hole $r \leq 2M$. Some examples of string trajectories illustrating these outcomes are shown in Fig. 2, where we plot the string radius $R = r \sin \theta$ (vertically) as a function of $Z = r \cos \theta$ (horizontally, string comes in from the left). In the three examples shown, the string is initially collapsed at a position a few horizon radii outside of the black hole. It then expands

and propagates to the right — towards the black hole. In Fig. 2a, the string passes the black hole but then returns and is captured, $r \leq 2M$. In Fig. 2b, the string passes the black hole and escapes to the right, $(r, \theta) = (\infty, \pi)$. In Fig. 2c, the string passes the black hole, then returns and finally escapes to the left, $(r, \theta) = (\infty, 0)$.

Besides the solutions with these three asymptotic outcomes, there is an infinite set of unstable periodic orbits, which separate the solutions with different asymptotic outcomes in the phase space of all solutions. Typical examples of periodic orbits are shown in Fig. 3. Besides the ones shown, there are also periodic orbits when the string starts a little further away from the black hole and oscillates a number of times before reaching it. There are no stable periodic orbits in our system.

To get a better understanding of the string dynamics, we now consider a two-dimensional slice of the four-dimensional space of initial conditions in more detail. It is most convenient to fix the constant “energy” E and then to impose one more relation between initial values of $(r, \theta, \dot{r}, \dot{\theta})$ at $\tau = 0$. Following the procedure of the basin-boundary method for chaotic scattering [9], we then color this two-dimensional slice of initial conditions according to the three different asymptotic outcomes mentioned above. Due to numerical reasons, the determination of the two asymptotic outcomes corresponding to escape is done not at infinity but at some large, but finite, value of r . While in general the string can pass this cutoff radius in one direction but change its mind later, for sufficiently large r , this procedure will only lead to a wrong color for very few points, as follows from the asymptotic behavior of the potential in the Hamiltonian (10) (this should be contrasted with the case of the mixmaster universe [16], where all the trajectories eventually bounce back).

In Fig. 4 we show examples of this coloring procedure applied to the phase space of string solutions. Fig. 4a and Fig. 4b show two different two-dimensional slices of the space of initial conditions. Fig. 4c and Fig. 4d show magnifications of the regions of Fig. 4b and Fig. 4c indicated in the previous figures. The boundaries between different colors in these figures correspond to the unstable periodic orbits. The magnifications of these so-called basin-boundaries reveal a fractal structure, see Figs. 4b-d. This provides the coordinate-invariant indication that the dynamics is in fact chaotic [9].

To get a quantitative measure we can also determine the fractal dimension. Consider for instance Fig. 4b, which corresponds to the two-dimensional slice in the space of initial conditions, given by

$$E = 14.0M, \quad \frac{d}{d\tau}(r \cos \theta) = 0 \text{ at } \tau = 0. \quad (11)$$

The box-counting dimension is defined by [9]

$$D = \lim_{\epsilon \rightarrow 0} \frac{\ln N(\epsilon)}{\ln(1/\epsilon)}, \quad (12)$$

where $N(\epsilon)$ is the number of squares of side length ϵ needed to cover the basin-boundary. A square should be counted only if it contains at least two different colors, otherwise it is not part of the basin-boundary. The result of this counting is shown as a plot of $\ln N(\epsilon)$ versus $\ln(1/\epsilon)$ in Fig. 5. The straight line is a least-square fit to the data points and shows that the dependence is indeed linear over the very wide range of resolution. The fractal dimension of Fig. 4b, calculated from the highest-resolution grid of 4000×3200 points, is

$$D = 1.65 \pm 0.03. \quad (13)$$

The non-integer value shows in a coordinate-invariant way [17] that the basin-boundary is indeed a fractal; a so-called strange repeller. The error in the result is due to the finite size of the numerical grid and slow convergence rate of definition (12), and can be estimated by examining D calculated at lower resolutions.

It is interesting to also examine the fractal dimension as a function of “energy” E . We considered the slice (11) in the energy range $E \in [0, 10^3 M]$ and computed the fractal dimension (12) of the basin-boundary (corresponding to Fig. 4b and its analog for different energies) as a function of energy E . The result is shown in Fig. 6, where we plot the fractal dimension D as a function of $\ln(E/M)$. For low energies, $E \lesssim 4.37M$, the dynamics is completely regular in the sense that there is only one asymptotic outcome — namely capture. For slightly larger energies, with values of E between $4.37M$ and $5.67M$, escape becomes possible but the different asymptotic outcomes are connected by “regular transitions”, corresponding to one-dimensional curves in the space of initial conditions (and thus corresponding to fractal dimension 1). However, at energy $E \simeq 5.67M$, the picture changes dramatically from regular to highly chaotic dynamics. In a very narrow energy range, the fractal dimension changes abruptly from 1 to approximately 1.6, whereafter it increases slightly for higher energies. It must be stressed that the numerical values given above for energies separating the different “phases” are slice-dependent. The phenomenon explained and demonstrated by Fig. 6 is however generic.

In conclusion, we have shown in a coordinate invariant way that the axially symmetric system of a circular test-string in the Schwarzschild black hole background is chaotic. Chaos sets in abruptly at a certain “critical” value of the external control parameter, which is related to the conserved energy of the string. Below this critical energy, the dynamics is regular. Above the critical energy, the dynamics is highly irregular and chaotic.

In all fairness, it should be mentioned that we have neglected some physical effects, including the backreaction and gravitational radiation of the cosmic string. However, the system considered here represents the simplest and most symmetric example of string dynamics in black hole spacetimes and therefore suggests quite generally that string dynamics in black hole spacetimes is chaotic (notice however that the problem of *stationary* strings in black hole spacetimes is completely integrable [18]). It would thus be interesting to consider other dynamical string configurations as well, and we notice that there has recently been some interest in the scattering and capture of open strings by a black hole; see Refs. [19,20] and references given therein.

ACKNOWLEDGEMENTS

We would like to thank V. P. Frolov and D. N. Page for stimulating discussions. This research was supported by the Natural Sciences and Engineering Research Council of Canada and by the Killam Trust.

REFERENCES

- [1] Hawking S W 1984 in *Relativity, Groups and Topology II* Les Houches Session XL (North Holland, Amsterdam)
- [2] Page D N 1984 *Class. Quantum Grav.* **1** 417
- [3] Cornish N J and Levin J J 1997 *Phys. Rev. D* **55** 7489
- [4] Dettmann C P, Frankel N E and Cornish N J 1994 *Phys. Rev. D* **50** 618
- [5] Cornish N J and Gibbons G W 1997 *Class. Quantum Grav.* **14** 1865
- [6] Carter B 1968 *Phys. Rev.* **174** 1559
- [7] Majumdar S D 1947 *Phys. Rev.* **72** 390
- [8] Papapetrou A 1947 *Proc. Roy. Irish Acad. A* **51** 191
- [9] Ott E 1993 *Chaos in Dynamical Systems* (Cambridge University Press, Cambridge)
- [10] Cornish N J 1997 E-print gr-qc/9709036
- [11] Vilenkin A and Shellard E P S 1994 *Cosmic Strings and other Topological Defects* (Cambridge University Press, Cambridge)
- [12] Misner C W, Thorne K S and Wheeler J A 1973 *Gravitation* (Freeman, San Francisco)
- [13] Larsen A L 1994 *Phys. Rev. D* **50** 2623
- [14] de Vega H J and Egusquiza I L 1994 *Phys. Rev. D* **49** 763
- [15] Press W H, Teukolsky S A, Vetterling W T and Flannery B P 1992 *Numerical Recipes* (Cambridge University Press, Cambridge)
- [16] Cornish N J and Levin J J 1997 *Phys. Rev. Lett.* **78** 998
- [17] Barnsley M F 1988 *Fractals Everywhere* (AP Inc, Boston)
- [18] Frolov V, Skarzhinski V, Zelnikov A and Heinrich O 1989 *Phys. Lett. B* **224** 255
- [19] De Villier J P and Frolov V 1999 *Class. Quantum Grav.* **16** 2403
- [20] Page D 1999 *Phys. Rev. D* **60** 023510

FIGURES

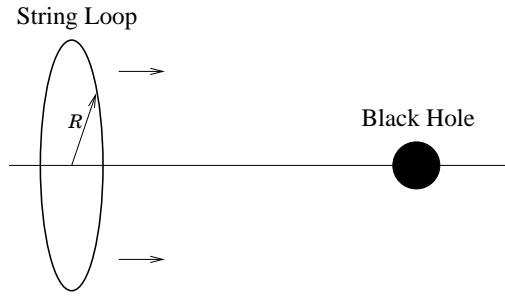


FIG. 1. Schematic illustration of string loop approaching black hole.

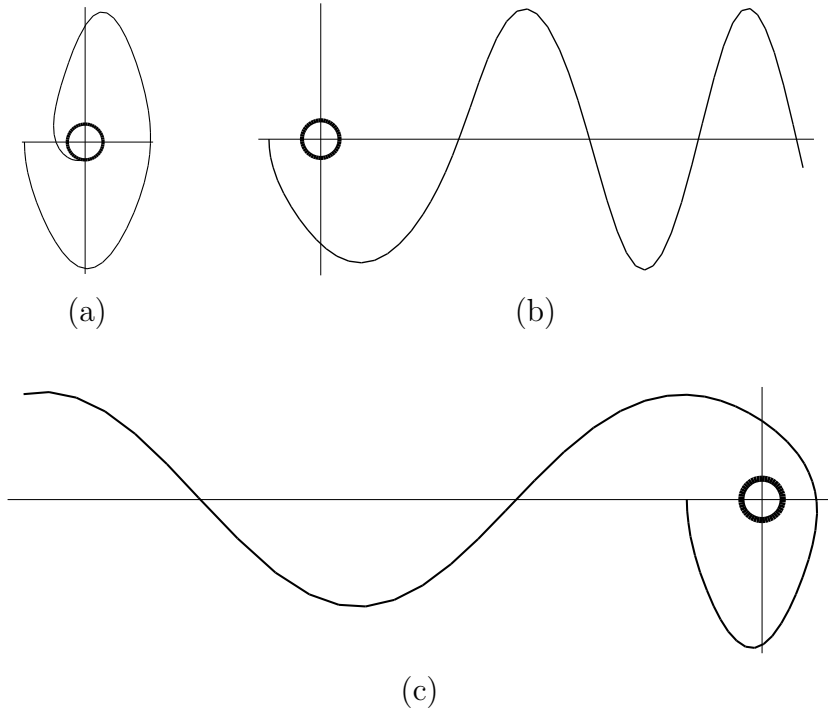


FIG. 2. Possible asymptotic outcomes of the string evolution: (a) capture, (b) escape, and (c) escape with backscatter. Axes are $(r \cos \theta, r \sin \theta)$, and the thick circle represents the event horizon of the black hole.

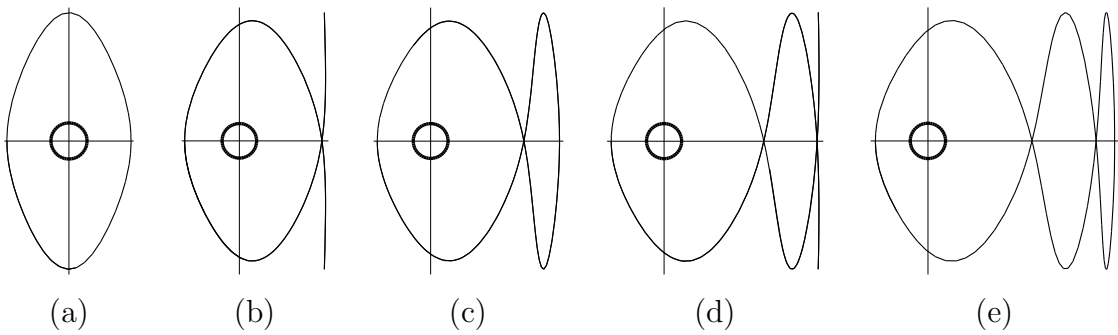
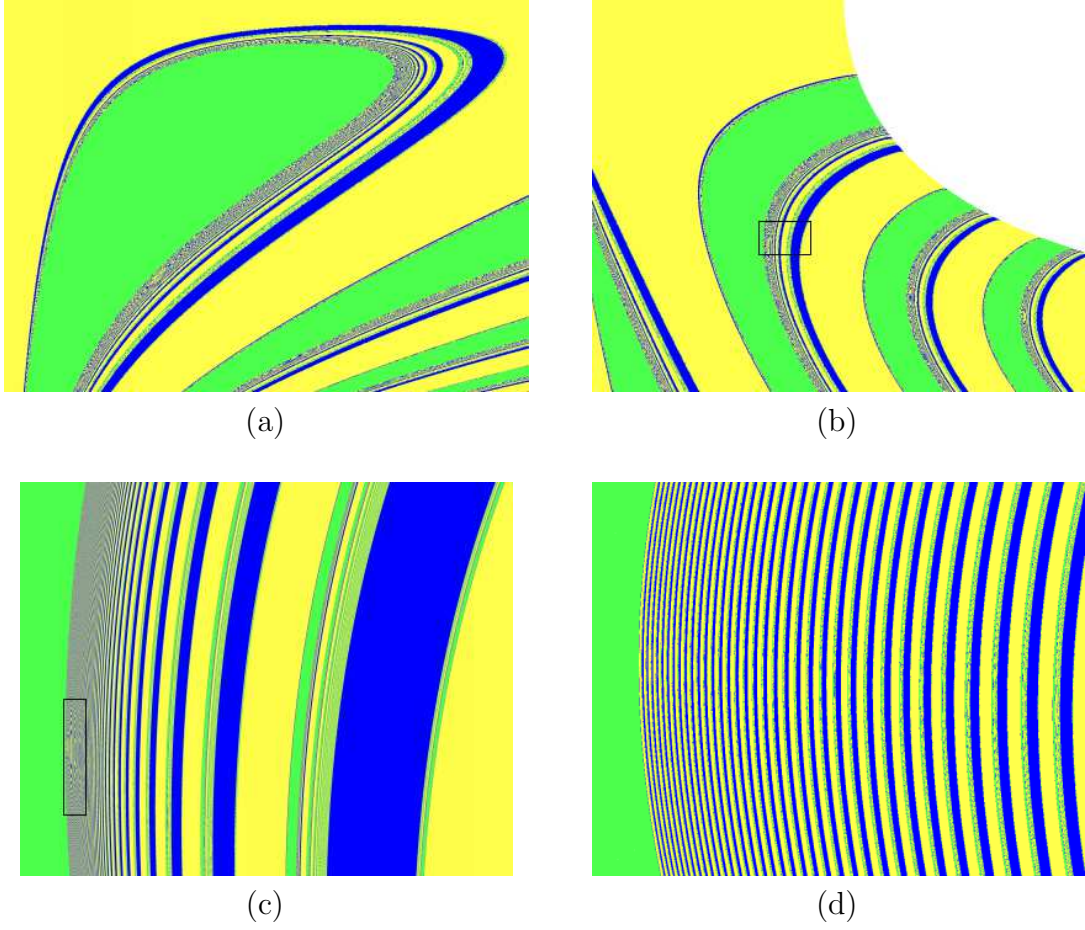


FIG. 3. Unstable periodic orbits.



Legend: ■ capture, ■ escape, ■ escape with backscatter.

FIG. 4. Basin-boundaries, plotted for $E = 14.0M$: (a) slice $\theta = 0$, with $r \in [2.0M, 29.2M]$ on horizontal axis, and $-\dot{r} \in [0, E]$ on vertical axis; (b) slice $\frac{d}{dr}(r \cos \theta) = 0$, with $r \in [2.0M, 27.5M]$ on horizontal axis, and $\theta \in [0, \pi/2]$ on vertical axis; (c) and (d) show fractal detail of figures (b) and (c) respectively.

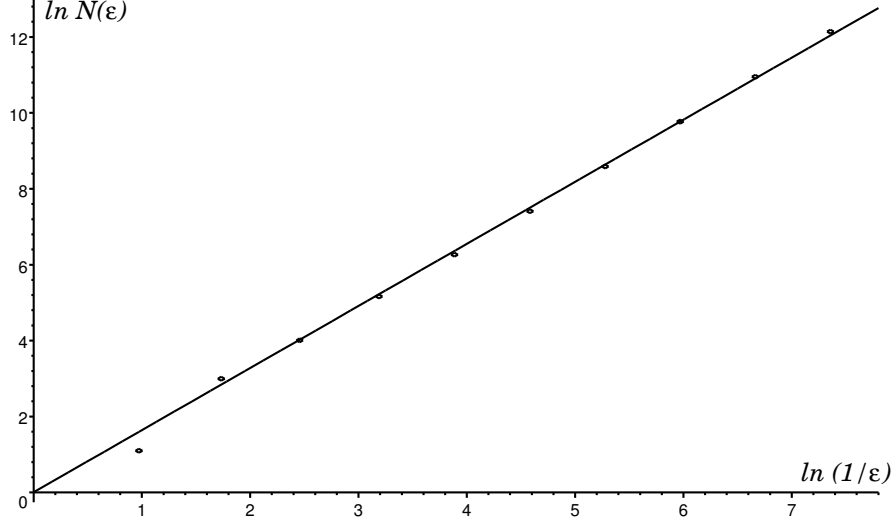


FIG. 5. Number of fractal points as a function of resolution, calculated for slice in Fig. 4b.

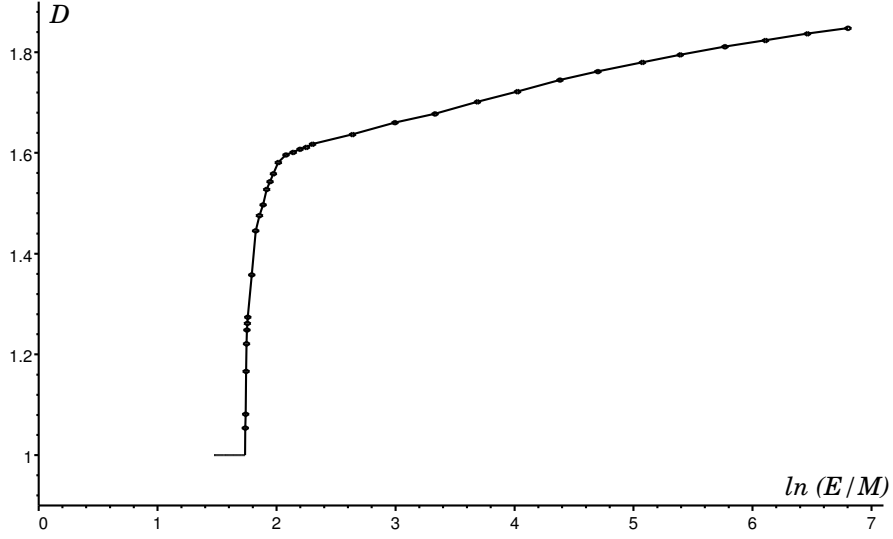


FIG. 6. Fractal dimension as a function of energy calculated for slice in Fig. 4b. Radial size of the box is scaled with energy as $r \in [2.0M, (2.0 + \frac{25.5}{14.0} \frac{E}{M})M]$ to keep the choice of the region consistent.